A multi-domain full-Stokes polarization modulator that is efficient for 300-2500nm spectropolarimetry

Frans Snik, Gerard van Harten, Andrey Alenin, Israel Vaughn, J. Tyo

SPIE.

A Multi-domain Full-Stokes Polarization Modulator that is Efficient for 300-2500 nm Spectropolarimetry

Frans Snik[a], Gerard van Harten[a,b], Andrey S. Alenin[c,d], Israel J. Vaughn[d], J. Scott Tyo[c,d]

[a]Sterrewacht Leiden, Universiteit Leiden, Niels Bohrweg 2, 2333 CA, Leiden, the Netherlands;
[b]now at: Jet Propulsion Laboratory, California Institute of Technology, Pasadena, CA 91109, USA;
[c]School of Engineering and IT, University of New South Wales Canberra, Canberra 2610 ACT, Australia;
[d]College of Optical Sciences, Univ. of Arizona, 1630 E. University Blvd., PO Box 210094, Tucson, AZ 85721-0094, USA.

ABSTRACT

We present the design and prototyping results for an ultra-wideband rotating polarization modulator that consists of a stack of quartz plates. The plate thicknesses and orientations were optimized such that after rotation of the modulator to 6 different angles before a polarization analyzer, the full Stokes vector can be optimally determined at all wavelengths from 300 to 2500 nm. Additional optimization parameters include minimal variation of the retardance with incidence angle and temperature, and the suppression of polarized spectral fringes for a spectral resolution of 10,000. The prototype modulator's design was re-optimized after the production and measurement of each individual quartz plate. We present the performance of the as-built prototype. To eliminate aliasing with inherent temporal variations of the source, the modulator can be used together with a polarizing beam-splitter ("dual-beam" approach). Because of the large sinusoidal spectral variations of the polarization modulation, this modulator can also be considered a "spectral modulator for channeled spectropolarimetry". Therefore, at each modulation state, spectrally resolved polarization information can also be extracted directly, although at limited spectral resolution. We use this modulator as an example of a "multi-domain polarization modulator", and outline a general approach for optimally storing polarization information in all available measurement dimensions (temporal, spatial, spectral), and rendering the overall polarization measurement independent from systematic effects in any of these dimensions.

Keywords: polarimetry

1. INTRODUCTION

In previous work,[1] we have introduced the design of a novel type of polarization modulation; a "polychromatic modulator". Originally targeted at implementation at an astronomical spectrograph, this step-wise rotating modulator offers full-Stokes spectropolarimetry over an extreme wavelength range of 300-2500 nm. In this communication, we recap the design considerations of this modulator, and discuss the performance of a prototype modulator, that was built through an iterative manufacturing approach. In the second half of this paper, we use this as-built modulator as a first example of a "multi-domain" modulator. Because the temporal modulation matrix is a strong function of wavelength, the modulator also provides snapshot quasi-sinusoidal spectral modulation for each of the temporal modulation states. We present a first exploration of spectral demodulation strategies for (continuum) polarization signals that vary slowly with wavelength. Using our polychromatic modulator as an example, we introduce the principles of a "multi-domain" modulator to measure the Stokes parameters for a certain target/scene, as a function of wavelength λ (or frequency σ), time, and/or spatial coordinates. Potential benefits of such a "multi-domain" polarization modulator include the trade-off of measurement bandwidths, and canceling/assessing degrading systematic effects.

---

email: snik@strw.leidenuniv.nl

2. POLYCHROMATIC MODULATOR DESIGN

Most current temporal modulators use achromatization (or even "super-achromatization"[2]) approaches to provide a large spectral bandwidth. However, as we aim to always observe spectrally resolved polarization signals, and as we aim to always measure all the Stokes parameters (as a function of wavelength), achromatization of the polarization modulation is actually not needed. As introduced in Ref.,[3] all that is required is an optimization of the *polarimetric efficiencies*[4] for all the Stokes parameters $\mathbf{S} = (I, Q, U, V)^T$, at every single wavelength, which is equivalent to minimizing the condition number of the modulation matrix at every wavelength.[5] This "polychromatic modulator" can therefore be very chromatic (a property that we will exploit in the second half of this paper).

Let the $n \times 4$ modulation matrix $\mathbf{O}$ describe the (temporal) modulation process of a full-Stokes modulator, which orientation and/or retardance is modified in n sequential steps, each corresponding to the same exposure time.

$$\mathbf{I}\left(\lambda\right) = \mathbf{O}\left(\lambda\right) \mathbf{S_{in}}\left(\lambda\right). \tag{1}$$

For a well-determined measurement, $n \geq 4$. The $4 \times n$ demodulation matrix $\mathbf{D}$ converts the measured intensities into a best measure for the Stokes parameters:

$$\mathbf{S_{meas.}}\left(\lambda\right) = \mathbf{D}\left(\lambda\right) \mathbf{O}\left(\lambda\right) \mathbf{S_{in}}\left(\lambda\right). \tag{2}$$

For $n = 4$, the corresponding demodulation matrix is the regular inverse of the modulation matrix. However, for $n > 4$ there are an infinite amount of demodulation matrices that fullfill $\mathbf{D}(\lambda)\mathbf{O}(\lambda) = \mathbf{I}$, with $\mathbf{I}$ the 4×4 identity matrix. To minimize the propagation of random noise, the optimum demodulation matrix is the Moore-Penrose pseudo-inverse:[4,5]

$$\mathbf{D}(\lambda) = (\mathbf{O}^T(\lambda)\mathbf{O}(\lambda))^{-1}\mathbf{O}^T(\lambda). \tag{3}$$

This optimal demodulation maximizes the combined polarization efficiencies, defined as:

$$\epsilon_i = \left(n \sum_{j=1}^{n} \mathsf{D}_{ij}^2 \right)^{-\frac{1}{2}}. \tag{4}$$

These efficiencies obey:

$$\epsilon_1 \leq 1, \qquad \sum_{i=2}^{4} \epsilon_i^2 \leq 1. \tag{5}$$

Therefore, for an optimally balanced full-Stokes modulator, the polarization efficiencies for Q, U, and V are $1/\sqrt{3}$. This number is to be compared with efficiencies of $1/\sqrt{2}$ for Q and U with a step-wise rotating half-wave plate polarimeter, and with an efficiency of 1 for V with a rotating quarter-wave plate polarimeter.

For the polychromatic modulator considered in this paper and introduced in Ref.[1] we have optimized a stack of quartz plates, such that after $n = 6$ modulation states (i.e. orientations with incremental $30°$ steps) the polarimetric efficiencies at every wavelength for the range 300–2500 nm for the obtained modulation matrix and resulting demodulation matrix cf. Eq.3 are:

$$\epsilon_1 \Rightarrow 1, \qquad \epsilon_{2,3,4} \Rightarrow \frac{1}{\sqrt{3}}. \tag{6}$$

With the optimization algorithm described in Ref.[3] we have designed a polychromatic modulator that consists of 4 quasi-zero order quartz retarders, each with its own effective retardance and orientation within the stack. The modulation matrix of this design is plotted in Fig. 2. Due to the degree of freedom in the modulation ($n = 6$) and the 8 degrees of freedom in the modulator design, the modulator reaches close-to-optimal efficiencies for all the Stokes parameters, and by employing quasi-zero order components, it could also be optimized to minimize the dependency of the modulation matrix on both incidence angle and temperature, to within tolerances.[1] Hence, this modulator can be implemented at an F/13 beam at normal incidence, at a temperature range of $\pm 5°C$

around room temperature. Moreover, the polarized spectral fringes due to polarization-dependent Fabry=Pérot etaloning inside the quartz crystals are suppressed to $< 10^{-4}$ for $R_\lambda = 10'000$.

In the special case where circular polarization can be neglected ($V \ll Q, U$), this modulation matrix can actually be reduced to a 3×3 matrix, which has a demodulation matrix from the trivial inverse. This is due to the fact that the modulation for linear polarization get repeated after $90°$. For cases with dominant circular polarization ($V \gg Q, U$), the modulation for purely Stokes V (and I), is a true beam-exchange (see Sect, 4.2), with the modulation changing sign after 3 steps.

3. POLYCHROMATIC MODULATOR PROTOTYPING

3.1 Manufacturing

A polychromatic modulator as described in Section 2, a stepped retarder for the 300–2500 nm wavelength range, has been manufactured by Bernhard Halle Nachfolger GmbH in Germany (see Fig. 1). The modulator consists of eight stacked quartz plates, each 15×15 mm square and about 0.5 mm thick. The plates are in optical contact to minimize internal reflections and the corresponding – generally polarized – spectral interference fringes. This way the strongest reflections will take place at the outer surfaces of the stack, at the interfaces between quartz and air. To suppress these reflections, a 200 nm-thick magnesium fluoride anti-reflection coating is applied to the front and back surface of the stack. The coating thickness is optimized such as to minimize polarized spectral interference fringes across the 300–2500 nm range. The modulator is fitted in a 1-inch threaded mount with the eight plates aligned; inside the plates the crystal axes are varied according to the design angles.

Manufacturing uncertainties in each of the eight plates can add up and significantly decrease the performance of the modulator. Moreover, different models of the birefringence and wavelength dispersion of quartz vary significantly, as shown in Ref.[6]. Following their work, we adopt an incremental manufacturing approach to limit the overall impact on the modulator, whilst relaxing manufacturing tolerances. Upon the production of each plate, its retardance and orientation are measured, and the design for the remaining plates is re-optimized. The measurements are performed by the manufacturer, with accuracies of 2 nm for the retardance at 546.1 nm, and 5 arcmin for the orientation of the crystal axis. The retardance of the first produced plate is measured across the 400–2400 nm wavelength range, showing agreement with the birefringence dispersion model from Ref.[7] to within the measurement uncertainty.

3.2 Experimental Verification

The manufactured polychromatic modulator is experimentally verified in the optical laboratory at Leiden Observatory. This involves the spectral measurement of the modulation matrix, derivation of the corresponding polarimetric efficiencies, and comparison to the design.

As shown in Section 2, the modulation matrix $\mathbf{O}(\lambda)$ describes how the modulator, when rotated in n steps in front of a fixed analyzer, modulates the transmitted intensity spectrum as $\mathbf{I}(\lambda)$ to encode the incoming Stokes vector $\mathbf{S}(\lambda)$, according to Eq. 1. To determine the modulation matrix, m known input polarization states are applied, the corresponding modulated intensities are measured, and the modulation matrix is solved for, according to:

$$\mathbf{O}(\lambda) = \mathbf{I}_{n \times m}(\lambda)\mathbf{S}_{4 \times m}^{-1}(\lambda), \tag{7}$$

with $^{-1}$ representing the Moore-Penrose pseudo-inverse.

The following efficient set of Stokes vectors, that is also practically producible across most of the 300–2500 nm wavelength range, is used for the verification of the polychromatic modulator:

$$\mathbf{S}_{4 \times 6}(\lambda) \approx \begin{pmatrix} 1 & 1 & 1 & 1 & 1 & 1 \\ 1 & -1 & 0 & 0 & 0 & 0 \\ 0 & 0 & 1 & -1 & 0 & 0 \\ 0 & 0 & 0 & 0 & 1 & -1 \end{pmatrix}. \tag{8}$$

The first four linear polarization states are created using a calcite Glan-Taylor polarizer at 0, 90, 45, and $-45°$, respectively. This polarizer exhibits an excellent extinction ratio of $\sim 10^{-5}$ across the transmitted wavelength

Figure 1. The manufactured polychromatic modulator for the 300–2500 nm wavelength range.

range of 400–2400 nm. The last two circular polarization states are created using the same polarizer at 0°, followed by a fused silica K-prism at 45 and −45°, which is transparent across the entire 300–2500 nm range. This type of retarder exhibits a high level of achromaticity because it is not based on birefringence, but instead it induces the quarter wave phase retardation using total internal reflections, like a Fresnel rhomb. The remaining chromaticity, as a result of the dispersion of the refractive index, is measured to be ≤ 0.04 waves, and is added to the model of Eq. (8).

The complete verification setup consists of the following components:

1. Halogen white light source.

2. Diaphragms allowing a 5 mm beam.

3. Calcite Glan-Taylor polarizer at 0, 90, 45, and −45°.

4. Fused silica K-prism quarter-wave retarder at 45 and −45°.

5. Polychromatic modulator at 0, 30, 60, 90, 120, and 150°.

6. Calcite Glan-Taylor analyzer at 0°.

7. Lens coupling light into fiber.

8. Optical fiber.

9. Fiber-fed spectrographs:

   - Visible: 180–880 nm range, 1 nm resolution.
   - Near-inrared: 1020–2640 nm range, 50 nm resolution.
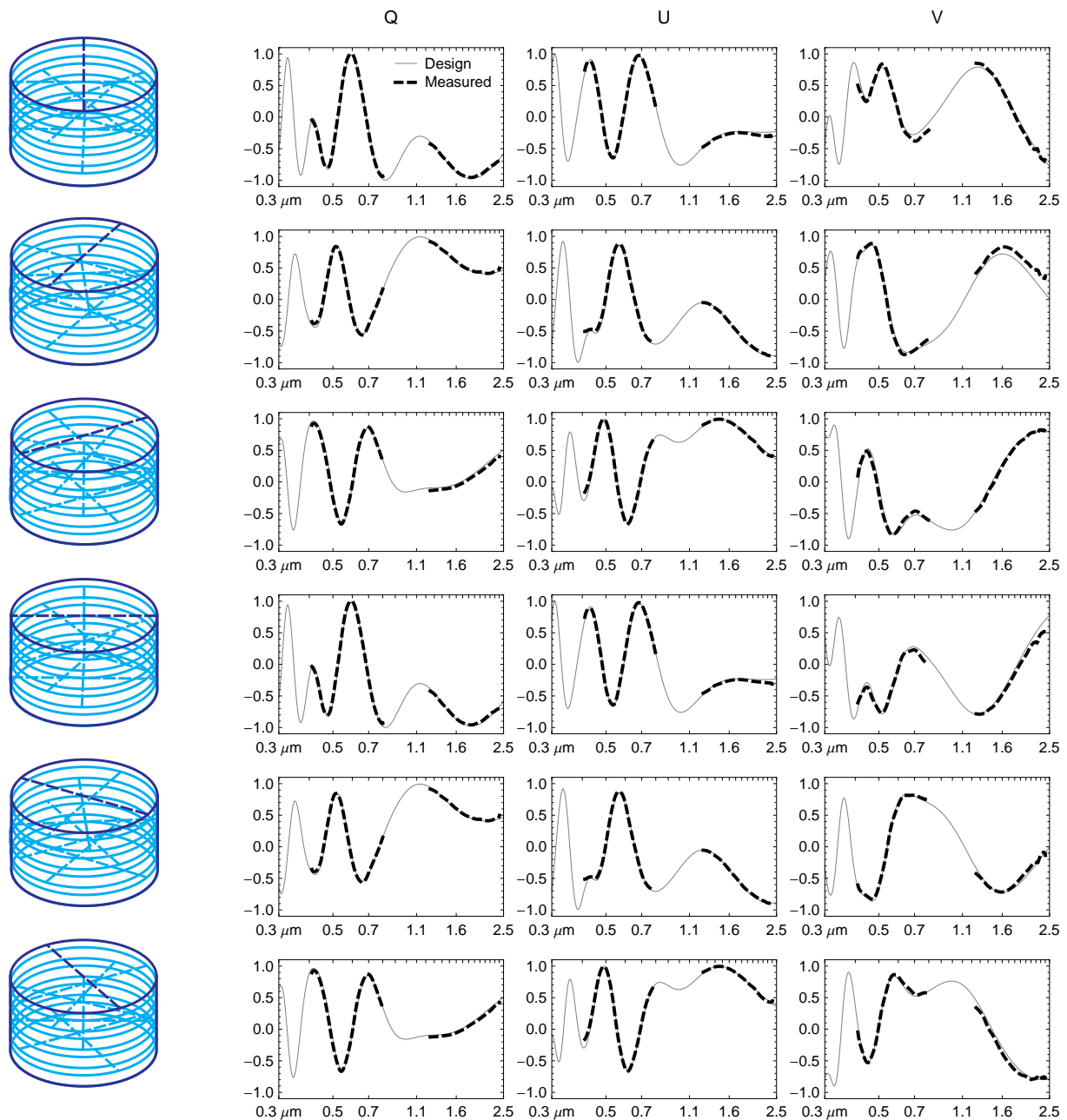
Figure 2. The designed (thin solid line) and measured (thick dashed line) modulation matrix as a function of wavelength for the polychromatic modulator consisting of four quasi zero-order quartz plates with different thicknesses and angular orientations. The first column of matrix elements pertaining to just Stokes I has been omitted. The elements of the modulation matrix for 300–400, 800–1200 and 2400–2500 nm were not measured, while the modulator's design is applicable at those wavelength ranges.

For each of the six input polarization states, the polychromatic modulator is stepped through its six angles, using a motorized precision rotation stage, and the corresponding spectra are measured with one of the two spectrographs; the scheme is repeated for the second spectrograph. The measured modulation matrix, normalized for intensity transmission, is shown in Fig. 2, along with the design matrix. Excellent agreement is found for
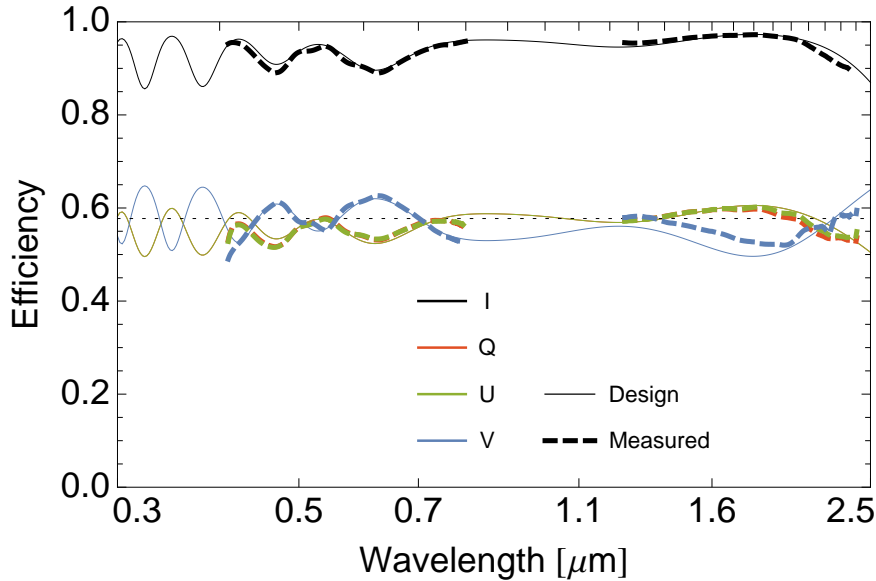
Figure 3. The designed (thin solid lines) and measured (thick dashed lines) polarimetric efficiencies as a function of wavelength for the polychromatic modulator consisting of four quasi zero-order quartz plates with different thicknesses and angular orientations.

all matrix elements across the entire measurable wavelength range within 400–2400 nm. The largest deviations occur in the near-infrared for circular input polarization, because of the low signal-to-noise ratio and high dark current of the near-infrared spectrograph, and the chromaticity of the K-prism retarder. Although the spectral deviation from a quarter-wave retardance is characterized in a separate measurement, errors in this measurement propagate to the derived modulation matrix. Moreover, a non-quarter-wave retardance reduces the amount of circular polarization to $< 100\%$, thus reducing the efficiency of the circular polarization verification measurement, and amplifying the propagation of measurement errors. Nevertheless, the excellent agreement in the modulation matrix, confirmed by the derived polarimetric efficiencies (see Fig. 3), shows the successful realization of a full-Stokes polychromatic modulator for at least the 400–2400 nm wavelength range.

4. MULTI-DOMAIN MODULATION CONSIDERATIONS

In the design of the polychromatic modulator, it has been assumed that the polarization signal is constant with time, at least during the modulation cycle of 6 steps, which for an astronomical spectropolarimeter may take many minutes. However, atmospheric fluctuations like turbulence ("seeing") and variable sky transmission generally introduce spurious polarization signals (that are potentially much larger than the often tiny polarimetric observable), if the polarimetric analyzer is a regular polarizer. Hence, many astronomical polarimeters contain a polarizing beam-splitter (in combination with a temporal modulator), that yields two beams with complementary yet instantaneous polarization information. A dual-beam polarimeter therefore provides cancellation of both the systematic effects in the time domain, as well as systematic differences (e.g. transmission, aberrations, residuals after detector calibration), to first order.[2,8] For rotating half-wave and quarter-wave plate polarimeters, the dual-beam demodulation can be performed through a double difference and a double ratio. Only the double difference demodulation is also fully applicable to polychromatic modulation:[2,9]

$$\frac{\mathbf{S}_{\text{mea.}}(\lambda)}{I_{\text{out}}(\lambda)} = \frac{1}{2} \left[\frac{\mathbf{S}_{\text{out},L}(\lambda)}{I_{\text{meas.},L}(\lambda)} - \frac{\mathbf{S}_{\text{out},R}(\lambda)}{I_{\text{out},R}(\lambda)} \right] . \tag{9}$$

The dual-beam implementation thus adds additional polarization information in another measurement domain("spatial"), to augment the merely temporal polychromatic modulation.

In this publication we open up a third polarization modulation domain: the spectral dimension. It is clear that for any of the 6 temporal modulation states in Fig. 2 there is a quasi-sinusoidal polarization modulation

as a function of wavelength, for all fractional polarized Stokes parameters $Q/I, U/I, V/I$. This implies that the polarization signal does not need to be constant with time, and that at every orientation of the modulator a snapshot full-Stokes spectropolarimetric measurement is obtained, although necessarily at degraded spectral resolution w.r.t. intrinsic resolution of the spectrometer. For an ultimate case of measuring $\mathbf{S}(\lambda, t)$ possibly even as a function of spatial coordinates $[x, y]$ or angular coordinates $[\theta, \phi]$, we aim to provide a framework for designing a true "multi-domain" polarization modulator. The complementarity in measurement domains should then optimize both the measurement accuracies and the bandwidths in all dimensions simultaneously.[10]

4.1 Spectral Modulation

Spectral polarization modulation (or "channeled spectropolarimetry")[11–16] is currently receiving a lot of attention and still undergoing significant development. The snapshot nature of spectral modulation not only furnishes time-resolved spectropolarimetry, but it also provides high intrinsic polarimetric sensitivity,[17] as no differential effects can degrade the polarimetric performance. The original configuration for spectral polarization modulation consists of two multi-order birefringent crystals with thickness ratio (1:2) at 0° and 45° orientation with respect to the polarization analyzer.[12, 13] This set-up yields three different spectral modulation period from which the complete Stokes vector can be obtained. An optimal implementation for just linear polarization ($Q/I, U/I$, or, equivalently, Degree and Angle of Linear Polarization, DoLP, AoLP) is found by combining an achromatic quarter-wave retarder with a single multi-order crystal retarder, such that a single spectral modulation carrier is created with its relative amplitude identical to the DoLP, and the phase of the modulation proportional to the AoLP.[15] In Ref.[16] a general framework for spectral modulation (channeled) spectropolarimetry is provided, with an orthogonal combination of any number of $\sin(n\sigma)/\cos(n\sigma)$ modulation carriers.

The most well-adapted demodulation strategy for spectral modulation lies in the Fourier plane,[11, 13] or utilizes the projection of the data on an orthogonal set of modulations.[16, 18] Alternative demodulation algorithms have been developed that fit a complete model (including the polarization spectra and non-ideal instrumental effects) to the acquired modulated intensity spectra and minimize an overall χ^2.[15, 19] Such an approach is conceptually fully equivalent to a large matrix pseudo-inversion cf. Eq. 3.

All current spectral modulation polarimeters offers modulations that are to a very large extent periodic in σ ($\propto 1/\lambda$), apart from a minor dispersion term in the birefringence of the multi-order retarder(s). It is clear from Fig. 2 that our polychromatic modulator is at best quasi-periodic in either σ or λ, and we need to extent the formalism for spectral demodulation.

4.2 Dual-Beam Polarimetry vs. Spatial Modulation

In the jargon of astronomical polarimetry, the use of a polarizing beam-splitter to provide a dual-beam system is sometimes called "spatial modulation".[2] The reason for this is that many astronomical targets have polarization signals that are constant in time. A linearly polarizing beam-splitter that yields two beams with intensities $\frac{1}{2}(I \pm Q)$ (provided identical transmissions). This is fully equivalent to a single-beam system with a temporal modulation half-wave plate at 0 and 45° orientation, which sequentially yields $\frac{1}{2}(I \pm Q)$. The combination of this temporal modulation and "spatial modulation" provides sufficient redundancy to cancel out differential systematic effects in time, and between the two beams ("in space").[2, 8] However, by rotating the half-wave plate to intermediate steps, a true sine-curve temporal modulation is achieved, whereas this is not possible for the spatial domain with just a polarizing beam-splitter. In the polarimetric remote sensing community, a beam-splitter implementation is therefore known as "division of amplitude" or "division of aperture" polarimeters,[20] or "space (or time) multiplexing" in contrast to a fully modulated system.

Also for spectral modulation, the dual-beam technique has proven valuable in canceling out systematic effects. The two spectra are fully complementary in their polarization modulation content (i.e. opposite phase), such that the sum of the two beams yields the regular intensity spectrum, and the difference normalized by the sum yields the pure polarization modulation.[15, 21] This technique allows for polarimetric demodulation that is fully free from aliasing with spectral intensity structure with Fourier components within the bandwidth of the spectral modulation. This normalization yields a modulation that is scaled between -1 and +1 and averaged around 0 that is ideally adapted to any linear algebra method for demodulation. If this signal has an average offset from 0 due to a transmission ratio $\neq 1$, the redundant polarization information in the two beams even allows for

a calibration of this transmission ratio from any actual data set itself.[15, 22] This means that the system can also be regarded as a regular but fully calibrated "division of amplitude" system, which can be demodulated at the *intrinsic spectral resolution* of the spectrometer. If one can make the assumption for a spectral modulator for linear polarization[15] that the AoLP varies smoothly (or not at all) with wavelength, one can even measure the polarization of spectral lines, which are much narrower than the typical modulation period.[22] In this way, a dual-beam implementation opens up polarimetric observables that are way outside the reach of polarimetric modulation inside a single dimension. This is not only valid for spectral modulation, but also for "true" spatial modulation and temporal modulation.

To generalize our multi-domain modulation approach, we will consider spatial modulations that can be expressed as an appropriately sampled combination of (quasi) sin/cos functions in the $[x, y]$ or $[\theta, \phi]$ dimensions. One such implementation is a micropolarizer array at the imaging detector ("division of focal plane"[20, 23]), with polarizers oriented at 0, 45, 90, 135° for different pixels. True sin/cos modulation can be furnished by implementations using wedged prisms or Sagnac interferometers based on Savart plates.[18, 24–27] Incidentally, many such implementations also provide a (slow) spectral modulation. One ideal spatial modulator could consist of an (achromatic) polarization grating.[28] This device is a patterned half-wave retarder, with its fast axis orientation linearly rotating as a function of one spatial coordinate. Located in a pupil plane location, this polarization grating produces spectra of order ± 1 that are oppositely circularly polarized. However, located in a focal plane (e.g. slit plane) location, it provides a perfect sine curve modulation of linear polarization as a function of one spatial coordinate. This achromatic polarization grating spatial modulator is actually conceptually interesting, as its modulation in the spatial domain is identical to the temporal modulation of a rotating half-wave plate, and the spectral modulation cf. Ref.[15] For each of these separate modulation implementation, the bandwidth in the respective domain is fully tunable. A combination of these three modulations would then yield an optimal multi-domain modulation for linear polarization. An additional dual-beam implementation with a polarizing beam-splitter could then supply an additional layer of recording of complementary polarization information, which can be used to cancel out systematics, and increase the bandwidths in any of the modulation domains.

4.3 Bandwidths

Throughout the polarization literature, the Stokes parameters are often assumed to be constant in order to make the linear algebra formalism applicable. In this paper, we make the (reasonable) assumption that the Stokes parameters are very slowly varying in time, and hence ignore temporal effects once the systematic variations have been accounted for through the dual-beam approach. However, in reality the Stokes parameters are varying in several independent domains including, but not limited to, space, time, wavelength, and angle of incidence. The amount of variability in each dimension is, in principle, completely independent, and hence the resolution (bandwidth) of the polarimeter provide a set of design parameters for the engineer.

The polychromatic modulator presented here was designed to provide essentially infinite polarization resolution in wavelength (limited only by the resolution of the spectrometer), while reducing the temporal resolution by a factor of at least six due to the time necessary to assemble the six measurements. However, as discussed later in Sect. 5, the nature of the polychromatic modulation itself provides some amount of polarization resolution in wavelength that has essentially infinite resolution in time (limited only by the temporal resolution of the measurement). Moving between these two extremes, one could imagine a system that uses two or three measurements and combined them in a wavelength-dependent way to produce a set of measurements that trades spectral and temporal resolution in a controlled way. In fact, it is possible for any or all of these strategies to be employed simultaneously by building multiple reconstruction kernels that can be used in post-processing. In this way, we have created the space-wavelength analog of the spatio-temporally modulated polarimeter of LaCasse[29, 30] or the space-wavelength modulated system of Oka.[31]

Vaughn et al.[32] have demonstrated that adding spatial modulation to a dual-rotating-retarder Mueller polarimeter by using a microgrid FPA produces a factor of nearly 3 increase in the *temporal bandwidth* of the instrument. It does that by changing the location of the information-carrying side bands in space-time Fourier space, providing greater space between these channels before aliasing and/or cross-talk occurs. In the future we will explore whether the spectral information obtained at each snapshot with the polychromatic modulator presented here can be leveraged to increase the temporal bandwidth of the final instrument.

4.4 Assessing Systematic Effects

In astronomical spectropolarimetry it has become common practice to implement an overdetermined temporal modulation (in combination with a dual-beam approach) to be able to assess the noise level, and the presence of (second-order) systematic effects that could induce false polarization signatures. For instance, for a regular polarimeter for measuring Stokes Q/I through temporal modulation, the half-wave plate would be incrementally oriented to 0, 45, 90, 135°, yielding an overdetermined 4×2 modulation matrix to yield I and Q. The demodulation for Stokes I is then manually chosen as $[\frac{1}{2}, \frac{1}{2}, \frac{1}{2}, \frac{1}{2}]^T$, and the demodulation for Stokes Q is then $[+\frac{1}{2}, -\frac{1}{2}, +\frac{1}{2}, -\frac{1}{2}]^T$, as it goes through modulation states $\frac{1}{2}(I + Q)$ and $\frac{1}{2}(I - Q)$ twice. The so-called "null spectra" for reference to the demodulated Q/I spectrum is obtained through the demodulation $[+\frac{1}{2}, -\frac{1}{2}, -\frac{1}{2}, +\frac{1}{2}]^T$ (or equivalent).[8] These null spectra are ideally identical to zero on a fraction polarization $(Q/I, U/I, V/I)$ plus the relevant noise. If any (second-order) systematic effects still propagate through the dual-beam demodulation, they can also be flagged in the null spectra, that are not "contaminated" by any real polarization signals.

For our polychromatic modulator, a similar approach to obtaining null spectra can be adopted for cases where $V \ll Q, U$ and $V \gg Q, U$, such that the column(s) for V or for Q, U, respectively, can be omitted. In that case, a "null demodulation" is obtained by flipping the signs on the second half of the pertinent rows in the demodulation matrix.

For the general full-Stokes case, it is not evident how to manually select such a "null demodulation", so we here introduce a generic approach given an overdetermined $(n \geq 5)$ modulation matrix (because for $n = 4$ there are no degrees of freedom to find any other demodulation that yields $I = 0$ than the solutions from the regular matrix inversion to find the demodulation matrix). We define our problem as follows (after normalization for Stokes I) to find a $4 \times n$ "null demodulation" matrix $\mathbf{N}(\lambda)$:

$$\mathbf{S_{null.}}(\lambda) = \mathbf{N}(\lambda)\,\mathbf{O}(\lambda)\,\mathbf{S_{in}}(\lambda) = \begin{pmatrix} 1 \\ 0 \\ 0 \\ 0 \end{pmatrix}. \tag{10}$$

The first row of $\mathbf{N}(\lambda)$ is identical to the first row of the regular demodulation matrix, as it should yield Stokes I in exactly the same way as in the regular demodulation process:

$$N_{1j}(\lambda) = D_{1j}(\lambda) \tag{11}$$

For any of the polarized Stokes parameters Q, U, V, corresponding to $i = 2, 3, 4$, respectively, we can write down a set of 4 equations to constrain the values in the respective rows of $\mathbf{N}(\lambda)$:

$$\sum_{j=1}^{n} N_{ij}(\lambda)O_{jk}(\lambda) = 0, \qquad k = 1, 2, 3, 4. \tag{12}$$

Because $n \geq 5$, we need at least one additional constraint for the null demodulation vector for each Stokes parameter $i = 2, 3, 4$. To impose a normalization that is identical to the regular demodulation for each Stokes parameter, we enforce

$$\sum_{j=1}^{n} N_{ij}^2(\lambda) = \sum_{j=1}^{n} D_{ij}^2(\lambda). \tag{13}$$

With this additional constraint, the "polarimetric efficiency" for the null demodulation becomes identical to the regular polarimetric efficiency for the demodulation to the Stokes parameter i, see Eq. 4. This means that for balanced full-Stokes efficiencies of $\sim 1/\sqrt{3}$, this set of equations provides the same constraints for the null demodulation related to Q, U, and V.

For our polychromatic modulator with $n = 6$ modulation states, the 5 coupled equations 12 and 13 still do not constrain the null demodulation matrix. We therefore need to adopt an additional constraint. One option is an additional normalization:

$$\sum_{j=1}^{n} |N_{ij}(\lambda)| = \sum_{j=1}^{n} |D_{ij}(\lambda)|. \tag{14}$$

Another option could be (balancing plusses and minuses):

$$\sum_{j=1}^{n} N_{ij}(\lambda) = 0. \tag{15}$$

The selected coupled set of equations is necessarily non-linear (because of Eq. 13), and therefore needs to be solved through an iterative numerical algorithm, which has $\mathbf{O}(\lambda)$ (and hence $\mathbf{D}(\lambda)$) as its input.

This concept of the "null spectrum" is closely related to the understanding of controlling the null space for modulated polarimeters.[33] When a signal is assumed to be constant in time, then the inversion operator can be constructed so that only certain spectra are used in the reconstruction. This allows the SNR to be enhanced, since the noise occupying these null spectra do not contribute to the noise in the final reconstruction. Diner et al.[34] leveraged this concept in the construction of their inversion operator by intentionally placing known sources of error (such as slow linear gradients) into the null space through their choice of the pseudo-inverse of the system operator. However, as the signal to be reconstructed begins to exhibit significant bandwidth, some of these degrees of freedom must actually be used to reconstruct the signal, and hence can no longer intentionally be placed in the null space of the operator. In this way, there is an inherent link between the necessary bandwidth, the system conditioning, and the resulting SNR.

5. SPECTRAL DEMODULATION

The prototyped polychromatic modulator was originally designed so that the instrument could function as a time-modulated polarimeter that has high polarimetric efficiency at every wavelength in the spectral range of interest. However, the device can also be used as a class of snapshot spectropolarimeter functioning as a channeled instrument. Instead of rotating the wave plate stack and taking several measurements in time at each wavelength, a single measurement a single spectrum can be thought of as a spectrally modulated polarimetric measurement since

$$X_{\phi}(\sigma) = A_0(\sigma)I(\sigma) + A_1(\sigma)Q(\sigma) + A_2(\sigma)U(\sigma) + A_3(\sigma)V(\sigma). \tag{16}$$

In Eq. 16, $X(\sigma)$ is the measured spectrum and A_0, A_1, A_2, and A_3 are the functions that are modulated by the Stokes parameters I, Q, U, and V, respectively. (Note that the numerical subscripts are chosen to coincide with the alternate $s_0 - s_3$ notation sometimes used to represent Stokes parameters).

Fig. 4 demonstrates that the spectral modulations for Q/I, U/I and V/I for the current polychromatic modulator design are already to a large extent orthogonal. This Figure also indicated that on a σ scale, the amount of Fourier components required to describe the modulation is $\lesssim 20$.

5.1 Snapshot measurement of spectrally flat Stokes Parameters

The functions $A_0(\sigma) - A_3(\sigma)$ are shown in Fig. 5 for $\phi = 0$ (the first temporal modulation state). In N wavelength measurements are made, and we assume that the Stokes parameters are not functions of wavelength (a dubious assumption), then we can construct a $N \times 4$ instrument matrix $\mathbf{W}$ that relates the modulations functions and the Stokes parameters to the measured irradiance at each wavelength. With the modulation functions shown in Fig. 5, the condition number of this matrix is 2.89, which reasonably well conditioned with the theoretical minimum of $\sqrt{3}$. The four rows of the pseudoinverse are also plotted in Fig. 5. If each row of the pseudoinverse is denoted as $P_k(\sigma)$, then we have

$$\int A_n(\sigma)P_m(\sigma)d\sigma = C\delta_{n,m}, \tag{17}$$

where σ is the wavenumber and C is a normalization constant.

This concept of using the spectrum as the measurements in a polarimeter is a slight variation on the channeled polarimeter (see Sect. 4.1). Previous work in this area used modulators that were made from high-order retarders, resulting in modulators that were pure sinusoids in wavenumber, unlike the quasi-periodic nature of the modulators shown in Fig. 5. Those truly periodic modulators create side bands the Fourier transform space of the spectrum (i.e. the interferogram or field autocorrelation sapce), which can be treated as orthogonal channels in the orthogonal frequency division multiplexing sense. The modulators of Fig. 5 also create channels, but these channels are not orthogonal in either spectral or interferogram space, so they need to be considered more fully.
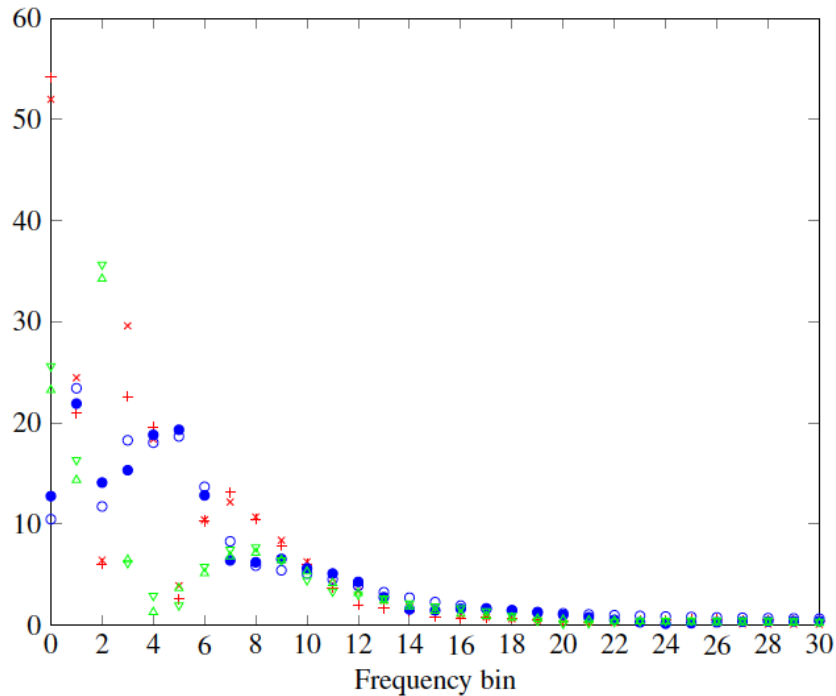
Figure 4. Fourier transforms (σ basis) of the spectral modulation functions for the first orientation in Fig.2. The different colors represent the different polarized Stokes parameters, as indicated in Fig. 5.

5.2 Spectral Bandwidth

In a conventional channeled spectropolarimeter, the spectral resolution of the spectrometer is used to measure these multiplexed channels, and hence the spectral resolution of the Stokes parameter measurements is reduced from that of the intensity measurement. Furthermore, "bandwidth" limitations are placed on the spectral variability of the Stokes parameters to prevent aliasing and/or cross-talk in the interferogram domain. Methods such as hybrid modulations (see Sect. 4.2) can be used to relax these limitations at the expense of requiring more measurements be made.

Since the modulation functions of our polychromatic modulator are not pure sinusoids, or even purely periodic, the concept of "bandwidth" is not obviously applicable. While we have demonstrated that zero-bandwidth (i.e. constant) Stokes parameters can be recovered from a single measurement, intuition suggests that some amount of variation in wavelength is permissible. Leaving the mathematical details for future work, we introduce three spectral basis sets for the polarization signals, on which parameters can be projected through a matrix pseudo-inversion process. An alternative demodulation approach consists of an overall χ^2 minimization of a comprehensive data model that contains a parametrization of the spectral polarization signals, the spectral modulation functions, and potential instrumental offsets, cf. Refs.[15,19] .

Consider the spectropolarimetric signal

$$\mathbf{S}(\sigma) = \left[\begin{array}{cccc} \sqrt{3}f(\sigma) & f(\sigma) & f(\sigma) & f(\sigma) \end{array} \right]^{\mathrm{T}}, \tag{18}$$

where $f(\sigma) = 1 - \cos(2\pi\overline{\sigma})$, and $\overline{\sigma}$ is a normalized variable $\overline{\sigma} = [0, 1]$ introduced for convenience.

5.2.1 Fourier Basis Set

As a first attempt, let's consider using Fourier coefficients as the basis set. This is, of course, the proper basis set to use in this case, since the signal is in terms of Fourier functions. However, in a real application, this would
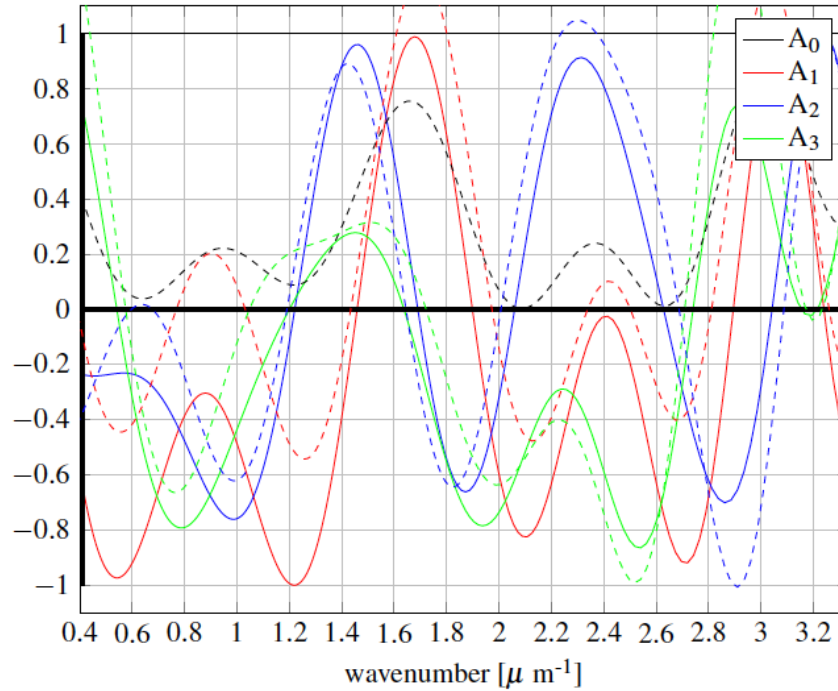
Figure 5. The spectral modulation functions (σ basis) for the first orientation in Fig.2, and their corresponding pseudo-inverse spectral demodulation functions.

not likely be known. In this case, our $\psi_s(\sigma)$ functions are

$$\psi_0(\sigma) = 1 \tag{19}$$
$$\psi_{2s-1}(\sigma) = \cos(s * \pi * \overline{\sigma}) \tag{20}$$
$$\psi_{2s}(\sigma) = \sin(s * \pi * \overline{\sigma}), \tag{21}$$

For intuitive reasons, we would generally like to use the smallest set of available basis functions that accomplishes the task. Furthermore, the interaction of the basis functions with the modulation functions must be considered. Fig. 6 shows the true signal along with the reconstructed signal using both three and five Fourier frequencies (a total of seven or 11 Fourier basis functions, respectively).

As can be seen, both representations present reasonable fidelity for the Stokes parameter spectra, at least for the first three Stokes parameters. The fidelity for V is notably worse. Furthermore, the accuracy of the model with fewer Fourier coefficients is actually better than that for the model with more coefficients. Even though the seven-frequency model has more degrees of freedom (17 singular values greater than 5% of the max compared with 14).

5.2.2 Wavelet Basis Set

A multi-resolution basis set might provide a compact representation in certain instances that could be useful. The simplest possible wavelet basis set is the Haar wavelet set.[35] This set allows reconstruction of piecewise-constant functions, but does its sampling on different scales. The advantage of a wavelet set over a nominally equivalent single-resolution set is that the latter can miss sampling parts of the waveform where the modulation function has a null (even if the waveform does not). However, the reconstructions in Fig. 7 are reasonably accurate.
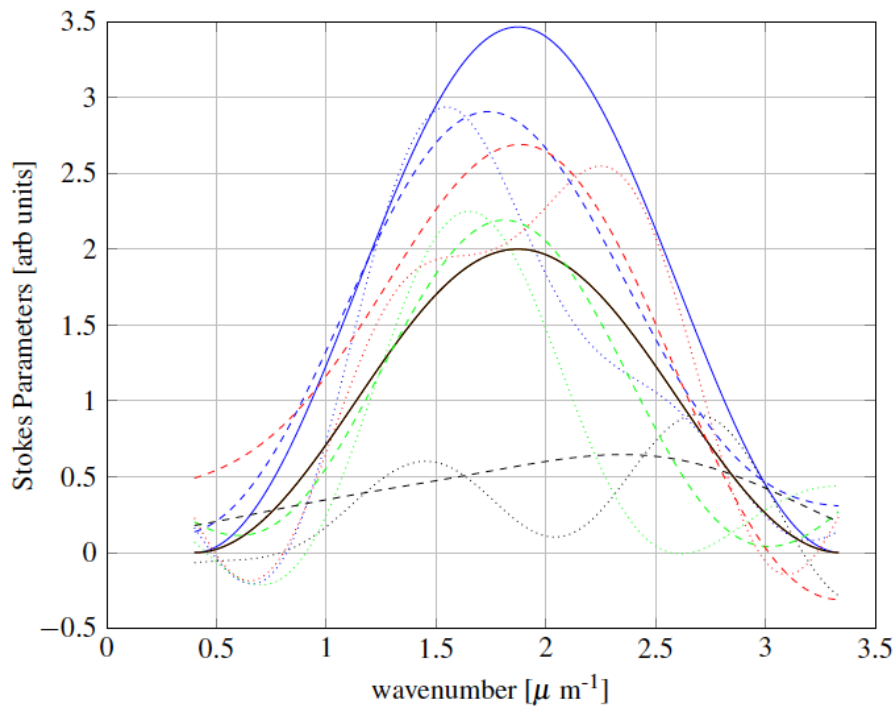
Figure 6. The true signal for I (blue solid) and Q, U, and V (red solid) along with the reconstructed signals for three (dashed) and five (dotted) Fourier frequencies. The blue curve is for I, green for Q, red for U, and black for V.

5.2.3 Gaussian Basis Set

The Fourier coefficients of the previous section have the potential disadvantage of being entire-domain. In certain instances, it might be preferably to use localized basis functions. As an example, consider defining N Gaussian functions that approximately cover the spectral range of interest

$$g_n(\sigma) = e^{-\pi\left(\frac{\sigma-\sigma_n}{1.33\Delta\sigma}\right)^2} \tag{22}$$

where σ_n are N evenly spaced wavenumber values with separation $\Delta\sigma$. The multiplier 1.33 was chosen somewhat arbitrarily to provide a reasonably smooth reconstruction. The reconstructed Stokes parameters for five (dashed) and 10 (dotted) Gaussian basis functions are shown compared with the ideal waveform for the Stokes parameters in Fig. 8.

5.3 Discussion

An interesting phenomenon occurs for all three classes of basis functions that are tested above. The quality of the reconstruction when using more basis functions can actually get worse. In each of the above examples, the smaller number of basis functions produced a more accurate reconstruction. The reason for this seems to be related to the question of bandwidth. The modulators shown in Fig. 5 have an inherent "frequency" to them, even though they are pseudoperiodic. The basis set chosen for reconstruction needs to vary more slowly than the modulator in order to be able to get reasonable fidelity. If an attempt is made to reconstruct more rapidly varying basis sets, the fitted coefficients are actually less accurate, even when the "proper" basis set is chosen (Fourier in this case). This requirement is basically a Nyquist-like limitation on the spectral resolution of the quasi-channeled system.

This analysis has demonstrated how the modulator waveforms can be used to make the system a snapshot spectropolarimeter. Just the the conventional channeled system has a bandwidth limitation introduced by the frequency of modulation, this quasi-periodic system has resolution limitations. Here we tested three arbitrary
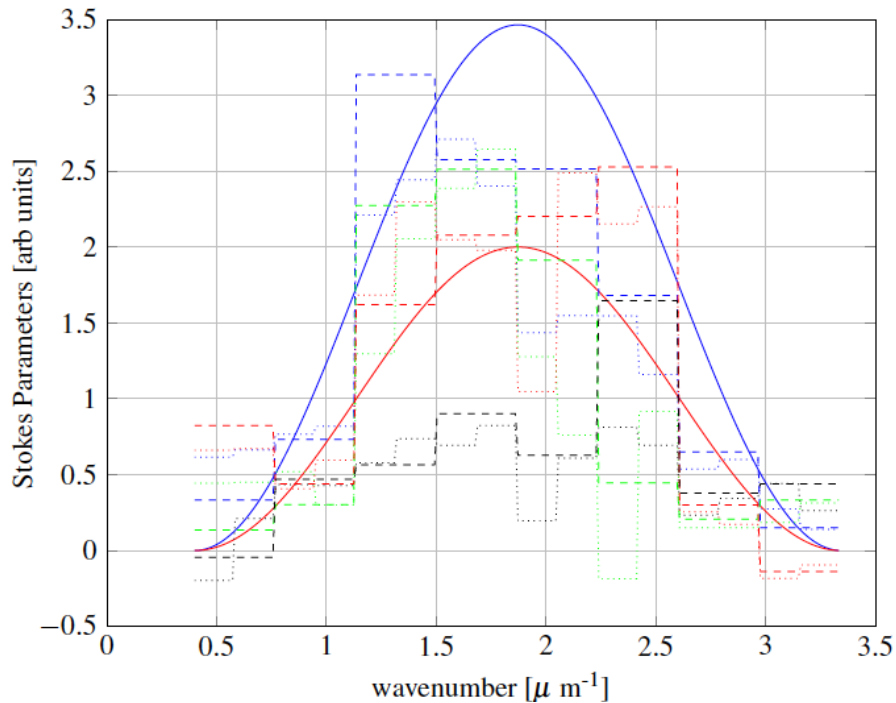
Figure 7. Reconstructed Stokes parameters for 8 (dashed) and 16 (dotted) Haar wavelet basis functions.

basis sets. However, it should be possible to choose a basis set that is optimized to perform with this particular set of modulators. Since the modulators are quasi-periodic, the reconstruction set might have different resolution in different portions of the spectrum. In order to find such a basis set, we will work to develop an optimization strategy that searches for well-conditioned reconstruction systems.

A second important point is to return to the concept of the "multi-snapshot" system posited by Alenin.[16] We already know that our polychromatic modulator can provide arbitrarily fine spectral resolution when used as a time-modulated instrument (i.e. ignoring the spectral channels completely). However, this requires four or six measurements, and introduces a corresponding temporal bandwidth limitation. In the future, we will investigate how the spectral and temporal resolution are traded off against each other as we move between treating the instrument as a channeled or a time-modulated device.

6. FUTURE WORK

- Increase spectral polarization modulation bandwidth by using higher-order retarders instead of the quasi-zero order quartz retarders that currently constitute the building blocks of our prototype polychromatic modulator.

- Introduce the formalism of optimizing polarimetric efficiencies to the spectral domain. We can adopt one set of efficiencies for the entire spectral range, but it may be preferable to cut this range up, and optimize the efficiencies for every (quasi-)period.

- Based on this novel formalism, we will optimize a new multi-domain modulator that has optimal polarimetric efficiencies in both the temporal and the spectral domains simultaneously.

- Elaborate the math for generic spectral demodulation through linear algebra, and find optimal basis functions.

- Define an optimal "null demodulation" matrix for this specific polychromatic temporal modulator.
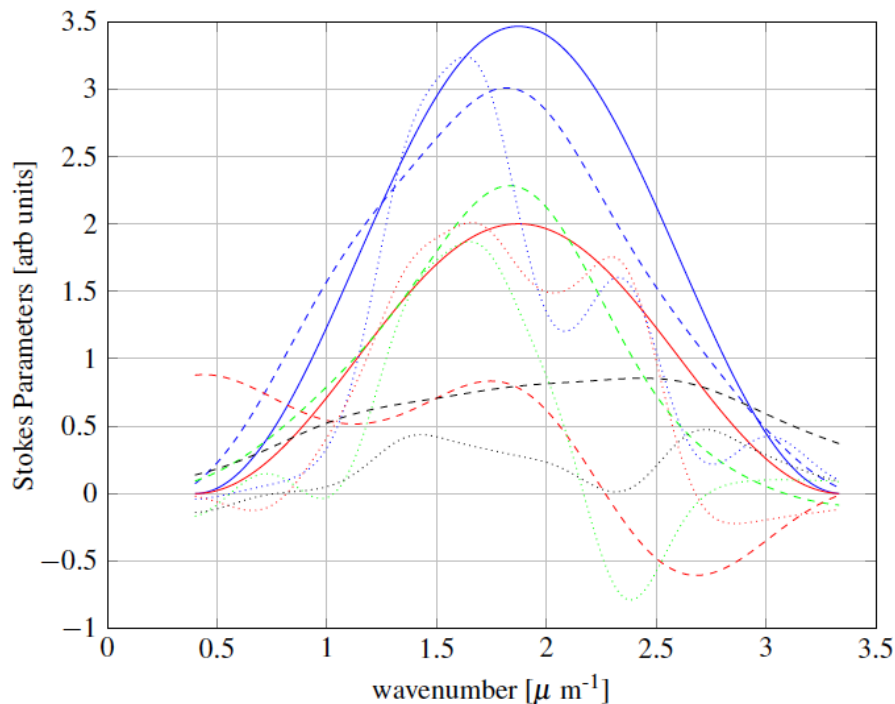
Figure 8. The ideal value for I (blue solid) and Q, U, and V (red solid) compared with the reconstructed Stokes parameters using five (dashed) and ten (dotted) Gaussian basis functions.

- Investigate instantaneous line polarimetry from spectral demodulation.[22]

- Investigate trading off bandwidths based on the properties of the target.

- Conceptually integrate "true" spatial modulation (in addition to the dual-beam implementation) to yield a complete (though perhaps academic) multi-domain modulation system to measure $\mathbf{S}(\lambda, t, x, y)$.

- Establish an overall multi-domain demodulation that simultaneously optimized polarimetric accuracy and bandwidth in all domains.

ACKNOWLEDGMENTS

REFERENCES

[1] F. Snik, G. van Harten, R. Navarro, P. Groot, L. Kaper, and A. de Wijn, "Design of a full-Stokes polarimeter for VLT/X-shooter," in *Society of Photo-Optical Instrumentation Engineers (SPIE) Conference Series*, *Society of Photo-Optical Instrumentation Engineers (SPIE) Conference Series* **8446**, Sept. 2012.

[2] F. Snik and C. U. Keller, "Astronomical Polarimetry: Polarized Views of Stars and Planets," in *Planets, Stars and Stellar Systems. Volume 2: Astronomical Techniques, Software and Data*, T. D. Oswalt and H. E. Bond, eds., p. 175, 2013.

[3] S. Tomczyk, R. Casini, A. G. de Wijn, and P. G. Nelson, "Wavelength-diverse polarization modulators for Stokes polarimetry," *Appl. Opt.* **49**, pp. 3580–3586, 2010.

[4] J. C. del Toro Iniesta and M. Collados, "Optimum Modulation and Demodulation Matrices for Solar Polarimetry," *Appl. Opt.* **39**, pp. 1637–1642, 2000.

[5] J. S. Tyo, "Design of optimal polarimeters: Maximization of signal-to-noise ratio and minimization of systematic error," *Appl. Opt.* **41**, pp. 619–630, Feb 2002.

[6] A.-B. Mahler, S. McClain, and R. Chipman, "Achromatic athermalized retarder fabrication," *Applied Optics* **50**, pp. 755–765, 2011.

[7] G. Ghosh, "Dispersion-equation coefficients for the refractive index and birefringence of calcite and quartz crystals," *Optics Communications* **163**, pp. 95–102, 1999.

[8] S. Bagnulo, M. Landolfi, J. D. Landstreet, E. Landi Degl'Innocenti, L. Fossati, and M. Sterzik, "Stellar Spectropolarimetry with Retarder Waveplate and Beam Splitter Devices," *PASP* **121**, pp. 993–1015, Sept. 2009.

[9] R. Casini, A. G. de Wijn, and P. G. Judge, "Analysis of seeing-induced polarization cross-talk and modulation scheme performance," *The Astrophysical Journal* **757**(1), p. 45, 2012.

[10] F. Snik, J. Craven-Jones, M. Escuti, S. Fineschi, D. Harrington, A. De Martino, D. Mawet, J. Riedi, and J. S. Tyo, "An overview of polarimetric sensing techniques and technology with applications to different research fields," 2014.

[11] M. Kudenov and D. Goldstein, *Channeled Polarimetry for Snapshot Measurements*. 2010.

[12] K. H. Nordsieck, "A Simple Polarimetric System for the Lick Observatory Image-Tube Scanner," *PASP* **86**, p. 324, June 1974.

[13] K. Oka and T. Kato, "Spectroscopic polarimetry with a channeled spectrum," *Opt. Lett.* **24**, pp. 1475–1477, Nov 1999.

[14] N. Hagen, K. oka, and E. L. Dereniak, "Snapshot Mueller matrix spectropolarimeter," **32**, pp. 2100 – 2102, 2007.

[15] F. Snik, T. Karalidi, and C. U. Keller, "Spectral modulation for full linear polarimetry," *Appl. Opt.* **48**, pp. 1337–1346, Mar 2009.

[16] A. S. Alenin and J. S. Tyo, "Generalized channeled polarimetry," *J. Opt. Soc. Am. A* **31**, pp. 1013–1022, May 2014.

[17] G. van Harten, F. Snik, J. H. H. Rietjens, J. M. Smit, J. de Boer, R. Diamantopoulou, O. P. Hasekamp, D. M. Stam, C. U. Keller, E. C. Laan, A. L. Verlaan, W. A. Vliegenthart, R. Ter Horst, R. Navarro, K. Wielinga, S. Hannemann, S. G. Moon, and R. Voors, "Prototyping for the Spectropolarimeter for Planetary EXploration (SPEX): calibration and sky measurements," in *Society of Photo-Optical Instrumentation Engineers (SPIE) Conference Series*, *Society of Photo-Optical Instrumentation Engineers (SPIE) Conference Series* **8160**, Sept. 2011.

[18] W. Sparks, T. A. Germer, J. W. MacKenty, and F. Snik, "Compact and robust method for full stokes spectropolarimetry," *Appl. Opt.* **51**, pp. 5495–5511, Aug 2012.

[19] G. van Harten, J. de Boer, J. H. H. Rietjens, A. Di Noia, F. Snik, H. Volten, J. M. Smit, O. P. Hasekamp, J. S. Henzing, and C. U. Keller, "Atmospheric aerosol characterization with a ground-based SPEX spectropolarimetric instrument," *Atmospheric Measurement Techniques* **7**, pp. 4341–4351, Dec. 2014.

[20] J. S. Tyo, D. L. Goldstein, D. B. Chenault, and J. A. Shaw, "Review of passive imaging polarimetry for remote sensing applications," *Appl. Opt.* **45**, pp. 5453–5469, Aug 2006.

[21] J. Craven and M. W. Kudenov, "False signature reduction in channeled spectropolarimetry," *Optical Engineering* **49**(5), pp. 053602–053602–10, 2010.

[22] G. van Harten, F. Snik, J. H. H. Rietjens, J. Martijn Smit, and C. U. Keller, "Spectral line polarimetry with a channeled polarimeter," *Applied Optics* **53**, p. 4187, July 2014.

[23] J. S. Tyo, C. F. LaCasse, and B. M. Ratliff, "Total elimination of sampling errors in polarization imagery obtained with integrated microgrid polarimeters," *Opt. Lett.* **34**, pp. 3187–3189, Oct 2009.

[24] K. Oka and T. Kaneko, "Compact complete imaging polarimeter using birefringent wedge prisms," *Opt. Express* **11**, pp. 1510–1519, Jun 2003.

[25] M. W. Kudenov, M. E. L. Jungwirth, E. L. Dereniak, and G. R. Gerhart, "White light sagnac interferometer for snapshot linear polarimetric imaging," *Opt. Express* **17**, pp. 22520–22534, Dec 2009.

[26] M. W. Kudenov, M. J. Escuti, E. L. Dereniak, and K. Oka, "White-light channeled imaging polarimeter using broadband polarization gratings," *Appl. Opt.* **50**, pp. 2283–2293, May 2011.

[27] J. Craven-Jones, M. W. Kudenov, M. G. Stapelbroek, and E. L. Dereniak, "Infrared hyperspectral imaging polarimeter using birefringent prisms," *Appl. Opt.* **50**, pp. 1170–1185, Mar 2011.

[28] C. Oh and M. J. Escuti, "Achromatic diffraction from polarization gratings with high efficiency," *Opt. Lett.* **33**, pp. 2287–2289, Oct 2008.

[29] C. F. LaCasse, T. Ririe, R. A. Chipman, and J. S. Tyo, "Spatio-temporal modulated polarimetry," 2011.

[30] C. F. LaCasse, R. A. Chipman, and J. S. Tyo, "Band limited data reconstruction in modulated polarimeters," *Opt. Express* **19**, pp. 14976–14989, Aug 2011.

[31] K. Oka, Y. Haga, and H. Michida, "Snapshot Mueller-matrix spectropolarimeter using spectral and spatial carriers," in *Society of Photo-Optical Instrumentation Engineers (SPIE) Conference Series*, *Society of Photo-Optical Instrumentation Engineers (SPIE) Conference Series* **9613**, 2015.

[32] I. J. Vaughn, O. G. Rodriguez-Herrera, M. Xu, and J. S. Tyo, "Bandwidth and crosstalk considerations in a spatio-temporally modulated polarimeter," in *Society of Photo-Optical Instrumentation Engineers (SPIE) Conference Series*, *Society of Photo-Optical Instrumentation Engineers (SPIE) Conference Series* **9613**, 2015.

[33] C. F. LaCasse, J. S. Tyo, and R. A. Chipman, "Role of the null space of the drm in the performance of modulated polarimeters," *Opt. Lett.* **37**, pp. 1097–1099, Mar 2012.

[34] D. J. Diner, A. Davis, B. Hancock, G. Gutt, R. A. Chipman, and B. Cairns, "Dual-photoelastic-modulator-based polarimetric imaging concept for aerosol remote sensing," *Appl. Opt.* **46**, pp. 8428–8445, Dec 2007.

[35] I. Daubecheis, *Ten Lectures on Wavelets*, ch. 3, pp. 53–106. SIAM, Philadelphia, PA, 1992.